Arch. Pharm. Chem. Life Sci. 2015, *348*, 1–13

ARCH PHARM
Archiv der Pharmazie

Full Paper

A New Series of Antibacterial Nitrosopyrimidines: Synthesis and Structure–Activity Relationship

Monica Olivella[1], Antonio Marchal[2], Manuel Nogueras[2], Manuel Melguizo[2], Beatriz Lima[3], Alejandro Tapia[3], Gabriela E. Feresin[3], Oscar Parravicini[4], Fernando Giannini[1], Sebastián A. Andujar[1,5], Justo Cobo[2], and Ricardo D. Enriz[1,5]*

[1] Facultad de Química, Bioquímica y Farmacia, Universidad Nacional de San Luis, San Luis, Argentina
[2] Departamento de Química Inorgánica y Orgánica, Universidad de Jaén, Jaén, Spain
[3] Facultad de Ingeniería, Instituto de Biotecnología, Universidad Nacional de San Juan, San Juan, Argentina
[4] Facultad de Bioquímica Química y Farmacia, Instituto de Química Orgánica, Universidad Nacional de Tucumán, S. M. de Tucumán, Argentina
[5] IMIBIO-SL (CONICET), San Luis, Argentina

New nitrosopyrimidines were synthesized and evaluated as potential antibacterial agents. Different compounds structurally related with 4,6-bis(alkyl or arylamino)-5-nitrosopyrimidines were evaluated. Some of these nitrosopyrimidines displayed significant antibacterial activity against human pathogenic bacteria. Among them compounds **1c**, **2a–c**, and **9a–c** exhibited remarkable activity against methicillin-sensitive and -resistant *Staphylococcus aureus*, *Escherichia coli*, *Yersinia enterocolitica*, and *Salmonella enteritidis*. A detailed structure–activity relationship study, supported by theoretical calculations, aided us to identify and understand the minimal structural requirements for the antibacterial action of the nitrosopyrimidines reported here. Thus, our results have led us to identify a topographical template that provides a guide for the design of new nitrosopyrimidines with antibacterial effects.

Keywords: Antibacterial compounds / 4,6-Bis(alkyl or arylamino)-5-nitrosopyrimidines / Conformational and electronic analysis / SAR

Received: July 7, 2014; Revised: September 2, 2014; Accepted: October 1, 2014

DOI 10.1002/ardp.201400271

Additional supporting information may be found in the online version of this article at the publisher's web-site.

Introduction

The continuous use of chemical antibiotics has led to the appearance of multi-resistant bacterial strains all over the world, which resulted in higher mortality on many infectious diseases [1–3]. Thus, the increasing resistance of pathogenic bacteria to conventional antibiotics has become a serious problem in health care, which requires alternatives to be developed. Medicinal chemists are still actively seeking new and improved antibacterial agents to combat the worrying ability of bacteria to acquire resistance to current drugs. Although combination therapy has emerged as a good alternative to bypass these disadvantages, there is a real need for a next generation of antibacterial agents [4–7].

In the course of our ongoing screening program for new antimicrobial compounds, we have previously reported antifungal [8–12] and antibacterial [13] activities of peptide compounds as well as of different molecules obtained from natural [14–17] and synthetic [18–23] sources. Among them, recently we reported a new series of compounds structurally related with 4,6-bis(alkyl or arylamino)-5-nitrosopyrimidines possessing a moderate antifungal effect against human pathogenic strains [24]. Compounds **2b**, **9b**, and **13** (see Section 2.1) exhibited antifungal activity against *Candida albicans*, *Candida tropicalis*, and *Cryptococcus neoformans*. From these results, we were intrigued to know if these compounds could also display antibacterial effect. Thus, in the

Correspondence: Dr. Ricardo D. Enriz, Facultad de Química, Bioquímica y Farmacia, Universidad Nacional de San Luis, Chacabuco 915, 5700 San Luis, Argentina.
E-mail: denriz@unsl.edu.ar
Fax: +54 02664 426367
*Additional correspondence: Dr. Justo Cobo,
E-mail: jcobo@ujaen.es

ARCH PHARM
Archiv der Pharmazie

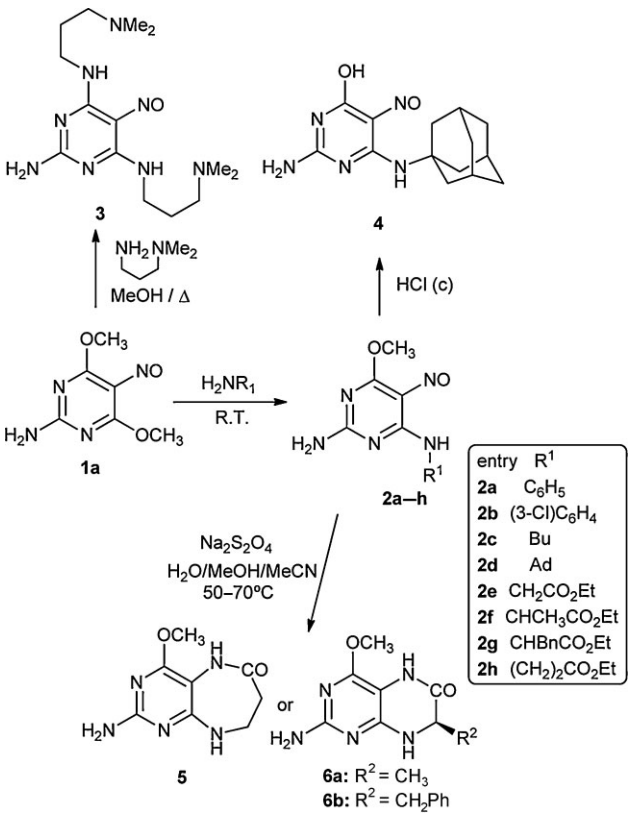

Scheme 1. Synthetic sequence for the preparation of 5-nitrosopyrimidines and fused pyrimidines via nitrosation-aminolysis from methoxypyrimidines.

present study, we use as starting structures those previously reported as the strongest antifungal compounds [24]. We tested these compounds against different pathogenic bacteria and some of them have displayed a strong antibacterial effect; therefore, we performed different structural modifications in this series in order to obtain a structure–activity relationship (SAR) as well as to determine the minimal structural requirements (a possible pharmacophoric pattern) to produce the antibacterial activity. In short, we here report the synthesis, antibacterial activities, and a SAR study, for a series of nitrosopyrimidine derivatives, most of them not described to date in the literature.

Results and discussion

Chemistry

In our aim of developing new bioactive pyrimidine-based compounds, we have optimized a three-step strategy consisting of a nitrosation, selective aminolysis of alkoxy groups, and a tandem reduction/cyclization [25–28]. In this fashion, we have already reported the synthesis of a family of N^4-substituted 2,4-diamino-6-methoxy-5-nitrosopyrimidines **2** by selective monoaminolysis of **1a** [25–27], which was prepared through the introduction of a 5-nitroso group to the commercial 2-amino-4,6-dimethoxypyrimidine (see Scheme 1 and Table 1).

An excess of amine on **1a** offered the N^4,N^6-disubstituted 2,4,6-triamino-5-nitrosopyrimidine **3**. We have also performed the hydrolysis of the methoxy group via acid catalysis of compound **2d** rendering the 5-nitrosopyrimidin-4(3*H*)one **4**.

On the other hand, if starting from those derivatives with an aminoester at C4 such as **2e–h**, the reduction of the nitroso group was followed by a spontaneous intramolecular cyclization through the ester group to render the fused pyrimidine derivatives either with pyrimidodiazepine nucleus such as **5** or with tetrahydropteridine structure such as **6**, as shown in Scheme 1.

In order to increase the structural diversity and also to test the influence of the alkoxy group, we have prepared the tetrahydropteridine analogs **8a–c** (Scheme 2), in a similar way to that described above, but changing the methoxy group at **1a** by a bulkier group, such as cyclohexylmethylenoxy by transalkoxylation.

Next, we exchanged the alkoxy and amino group position in the starting material and so from **1c** several *N*-substituted diamino and triamino-5-nitrosopyrimidine derivatives, such as **9** and **10** (Scheme 3) (isomers to previously synthesized 5-nitrospyrimidines), were prepared in a similar procedure [26].

Finally, several pyrimidine derivatives with different alkoxy or thioalkyl groups, namely **11–15** (Fig. 1), were prepared in order to test their activity in comparison with the active nitrosopyrimidine **1c** [25, 29].

Table 1. Structural features of compounds 9 and 10.

Compounds type 9			Compounds type 10		
Entry	**R^1**	**R^2**	**Entry**	**R^1**	**R^2**
9a	Bu	H	**10a**	Bu	H
9b	C_6H_5	H	**10b**	C_6H_5	H
9c	(3-Cl)C_6H_4	H	**10c**	(3,4-OMe)$C_6H_4CH_2$	H
9d	$C_6H_5CH_2$	H	**10d**	$(CH_2)_2$–OH	H
9e	(3,4-OMe)$C_6H_4CH_2$	H	**10e**	$(CH_2)_2$–OH	$=R^1$
9f	–$(CH_2)_4$–				

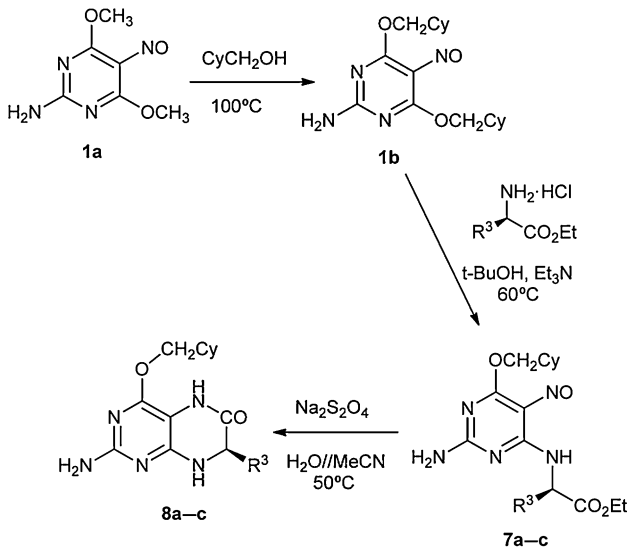

7a, **8a**: R^3 = H; **7b**, **8b**: R_3 = CH_3; **7c**, **8c**: R^3 = CH_2Ph

Scheme 2. Preparation of pteridine analogs including cyclohexylmethylenoxy group.

Antibacterial activity and SARs

For this study, we chose as starting structures compounds **2b**, **9b**, and **13**, which were reported as the most active compounds against *C. albicans*, *C. tropicalis*, and *C. neoformans* in our previous paper [24]. As expected, these compounds displayed a strong antibacterial activity against all the species tested except *Pseudomonas aeruginosa*

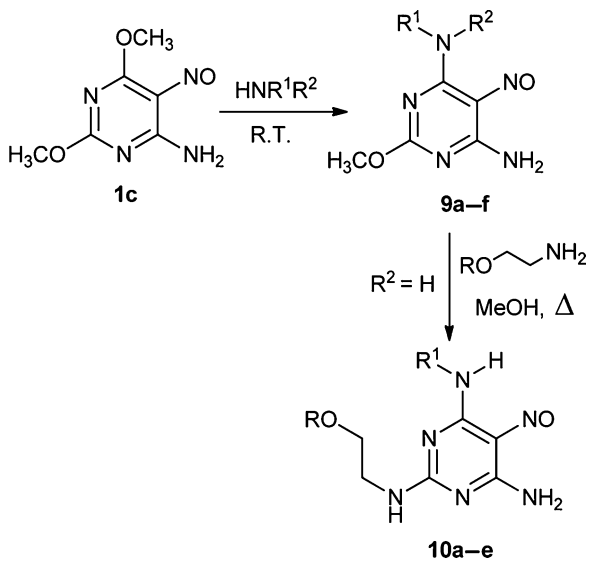

Scheme 3. Preparation of some N^2,N^4-disubstituted 2,4-diamino-5-nitrosopyrimidines **9** and **10**.

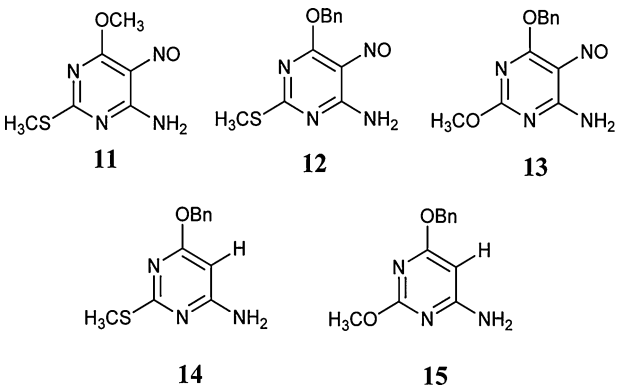

Figure 1. Structures of compounds **11**–**15**.

ATCC27853 (Table 2). The three compounds showed similar antibacterial activities with MIC values ranging from 0.1 to 2.5 μg/mL (Table 2). It should be noted that the antibacterial activities obtained for these compounds are stronger than those attained acting as antifungal agents [24].

In the next step of our study, we performed different chemical modifications on these three compounds in order to obtain an SAR, which could help us to understand a possible pharmacophoric patron for this series. Thus, we synthesized and tested 35 compounds structurally related with compounds **2b**, **9b**, and **13**; such compounds have been described in the previous section (compounds **1**–**15**).

To evaluate the SARs, the effects of structural changes on the general structure shown in Fig. 2 were considered; thus, we performed different substitutions at R^1, R^2, and R^3. Several compounds showed strong antibacterial activities in this series, of which the most prominent are **2a**–**c**, **9a**–**e**, and **13**. It should be noted that the active compounds displayed significant antibacterial effects against all the bacteria tested here except against *P. aeruginosa*. Unfortunately, none of them show any activity against this specie, but many compounds were active against methicillin-resistant *Staphylococcus aureus*.

Thirty-five compounds were evaluated against Gram-(+) and Gram-(−) bacteria. The compounds type **9** (**a**–**e**) and compounds **11**–**13** exhibited remarkable antibacterial activity against methicillin-sensitive and -resistant *S. aureus*, *Escherichia coli* ATCC, and clinical isolate, *Yersinia enterocolitica*, *Salmonella enteritidis* and LM-*S.* sp., with MIC values between 0.5 and 15 μg/mL, while the compounds type **2** (**a**–**c**) were stronger active against the same strains except against *Staphylococcus aureus* (mr) and *Yersinia enterocolitica* (MIC = 40 and MIC = 50 μg/mL).

Regarding the influence of the substituents on R^1, R^2, and R^3, it appears that the presence of a group possessing properties to produce hydrogen bonds (either acting like donor or acceptor of protons) is necessary to produce the antibacterial effect. It should be noted that all the active compounds possess NH_2 or OCH_3 groups at R^1 or R^3 indistinctly. In fact in these

Table 2. Antibacterial activity of the nitrosopyrimidine compounds.

Comp.	MIC[a] (μg/mL)								
	Sa (ms)	Sa (mr)	Ec	LM_1-Ec	LM_2-Ec	Pa	PI-Ye	MI-Se	Ssp (LM)
1b	>50	>50	>50	>50	>50	>50	>50	>50	>50
1c	5	2.5	2.5	12.5	2.5	>50	30	2.5	2.5
2a	>50	0.5	5	>50	5	>50	>50	0.5	2.5
2b	40	0.5	5	>50	5	>50	40	1	2.5
2c	40	0.5	6.25	12.5	5	>50	50	5	5
2d	>50	>50	>50	>50	>50	>50	>50	>50	>50
2e	25	50	10	10	10	>50	25	25	25
2f	20	50	20	12.5	40	>50	30	40	20
2g	40	>50	40	>50	40	>50	40	40	40
2h	>50	>50	>50	>50	>50	>50	>50	>50	>50
3	>50	>50	>50	>50	>50	>50	>50	>50	>50
4	>50	>50	>50	>50	>50	>50	>50	>50	>50
5	>50	>50	>50	>50	>50	>50	>50	>50	>50
6a	>50	>50	>50	>50	>50	>50	>50	>50	>50
6b	>50	>50	>50	>50	>50	>50	>50	>50	>50
7b	25	>50	>50	>50	30	>50	>50	>50	>50
8a	>50	>50	>50	>50	>50	>50	>50	>50	>50
8b	>50	>50	>50	>50	>50	>50	>50	>50	>50
8c	>50	>50	>50	>50	>50	>50	>50	>50	>50
9a	6.25	2.5	6.25	12.5	5	>50	50	5	5
9b	1.25	5	1	1	1	>40	1	0.5	1
9c	0,5	1	1	2.5	1	>50	0.5	2.5	5
9d	15	2.5	1	6.25	2.5	>50	1	5	5
9e	2.5	2.5	15	25	5	>50	25	0.5	1
9f	>50	>50	>50	>50	>50	>50	>50	>50	>50
10a	>50	>50	>50	>50	>50	>50	>50	50	>50
10b	>50	>50	>50	>50	>50	>50	>50	>50	>50
10c	>50	>50	40	50	50	>50	50	>50	50
10d	>50	>50	40	50	50	>50	50	>50	50
10e	>50	>50	>50	>50	>50	>50	>50	>50	>50
11	2.5	2.5	2.5	12.5	3.25	>50	6.25	2.5	2.5
12	12.5	1	2.5	6.25	2.5	>50	5	1	2.5
13	12.5	1	2.5	6.25	2.5	>50	2.5	1	2.5
14	>50	>50	>50	>50	>50	>50	>50	>50	>50
15	>50	>50	>50	>50	>50	>50	>50	>50	>50
Cef[b]	0.5	0.5	0.5	5	0.5	7.5	0.5	12.5	0.5

[a] The minimal inhibitory concentration (MIC) of the peptides were determined ($n = 3$) for Sa (ms): *Staphylococcus aureus* methicillin-sensitive ATCC 29213, Sa (mr): *Staphylococcus aureus* methicillin-resistant ATCC 43300, Ec: *Escherichia coli* ATCC 25922, LM_1-Ec: LM1-*Escherichia coli*, LM_2-Ec: LM2-*Escherichia coli*, Pa: *Pseudomonas aeruginosa* ATCC 27853, PI-Ye: PI-*Yersinia enterocolitica*, MI-Se: MI-*Salmonella enteritidis*, Ssp (LM): *Salmonella* sp. (LM).
[b] Cefotaxime.

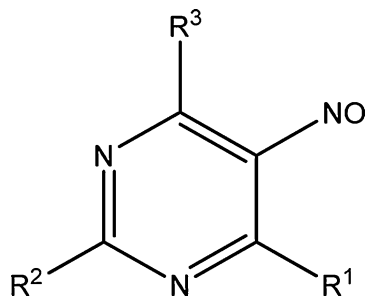

Figure 2. General structure of the nitrosopyrimidine compounds analyzed here.

compounds when NH_2 is located at R^1, then OCH_3 group is at R^3 and vice versa. On the other hand, noting the structures taken as a starting point (compounds **2b**, **9b**, and **13**) it would be reasonable to think that the presence of a second aromatic ring is necessary to produce the antibacterial effect. Such idea is reinforced when we observe the strong activities obtained for compounds **2a** and **9c–e** (Table 2). However, the replacement of phenyl group by butyl was well tolerated, keeping the antibacterial activity (observe activities of compounds **2a** and **2c**). A similar result was observed for compounds **9a** and **9b**. These results clearly indicate that in the presence of a second aromatic ring, it is not a structural requirement to produce the biological response. However, it

is also important to note that not any group is operative in this position since if this group becomes more polar, the antibacterial activity is lost. This can be seen comparing the activities obtained for compounds **2e–h** with **9b**. On the other hand, the replacement of the aromatic ring in compound **9b** by an adamantyl group (compound **2d**) gives a compound devoid of any antibacterial effect indicating that not any hydrophobic substituent at R^2 is operative for these compounds. In addition, when we performed significant structural modifications simultaneously on R^1 and R^2, we observed a near-total loss of the activity (compounds **1b**, **3**, **7a**, **8a–c**, **9f**, and **10a,d**).

Using the concept of homology, compound **9d** was synthesized, which is the higher homolog of **9b**. This compound showed a very similar antibacterial activity to that of **9b**. Similar activities were also obtained for **9c**, which is a structural analog of **9b**. Thus, these results indicate that an extra methylene group is well tolerated in the connecting chain of the aromatic rings for these compounds.

At this point of our study, we were interested to determine the pharmacophoric patron of this series and to achieve this we conducted a molecular simplification. By applying the concept of molecular disjunction, we obtained compound **1c**. This compound showed a strong antibacterial activity being the simplest structure that retains this effect. It should be noted that compound **1c** is a molecular simplification of **13** in which the *O*-benzyl group has been replaced by OCH_3. Once the simplest structure with antibacterial activity of this series was obtained, we applied the concept of isosterism by replacing SCH_3 by OCH_3. Thus, we obtained compound **11**, which showed an antibacterial effect similar to **1c**. The same molecular modification was also applied on compound **13** and in this case, we obtained compound **12**, which also presented a strong antibacterial activity.

In the next stage of our study, we wanted to find out if the presence of the NO group was a necessary requisite for the antibacterial activity of this series. Thus, other modification that was done was to remove this group replacing it by H. From compounds **12** and **13**, we obtained **14** and **15**, respectively; both compounds were completely inactive indicating that the presence of NO group is a structural requirement necessary to produce antibacterial activity. Cyclic compounds **5**, **6a**, **6b**, **8a**, **8b**, and **8c** give an additional support to this observation. It is clear however that the mere presence of the NO group is not sufficient to produce the biological effect because many compounds possessing this group were inactive.

Having in mind the potential limitations that could present these compounds because of possible toxicities they may display, we performed an acute toxicity study for those derivatives that showed major antibacterial activities. We observed that compound **13** and its structurally related derivative **12** exhibited high acute toxicity (2.5 μg/mL both compounds), which severely limits their applicability as antibacterial agents. These results are in agreement with those previously reported for nitrosopyrimidine derivatives acting as antifungal agents [24]. On the other hand, although **1c** and **9a** showed potent antibacterial activity, at the same time these compounds displayed a relatively significant acute toxicity (7.5 and 10 μg/mL, respectively), which does not allow to have a wide margin between the concentration required to produce antibacterial activity and the concentration at which it begins to be toxic. In contrast to these results, the compounds that showed a good relationship between the concentrations in which they display antibacterial activity with respect to those having toxicity were **2a**, **2b**, **9b**, **9c**, and **9e**. In fact, these compounds showed no acute toxic effects at least at concentrations above 50 μg/mL. It is important to note that we did not measure toxic effects at higher concentrations than those reported here and therefore, it might be expected that these compounds display such effects at substantially higher concentrations.

To confirm the results obtained from the acute toxicity study, we performed a study of cytotoxicity of three representative compounds of this series (compounds **2a**, **2b**, and **13**) using the well-known MTT bioassay. We have previously used this technique successfully to the study of other compounds of biological interest [30, 31].

Figure 3 shows the cytotoxic effects obtained for compounds **2a**, **9b**, and **13** using the HepG2 cell culture. Compound **13** displays a high cytotoxicity against hepatocytes even at relatively low concentrations. In contrast, compounds **2a** and **9b** showed a moderate cytotoxicity at least until 32 mg/mL. These results are in agreement with those obtained by the acute toxicity test.

From the results of these exploratory and preliminary studies, we cannot discard the putative inconvenience of these compounds as lead structures. However, it should be noted that compounds reported here constitute a set of candidate structures, which has been evaluated considering

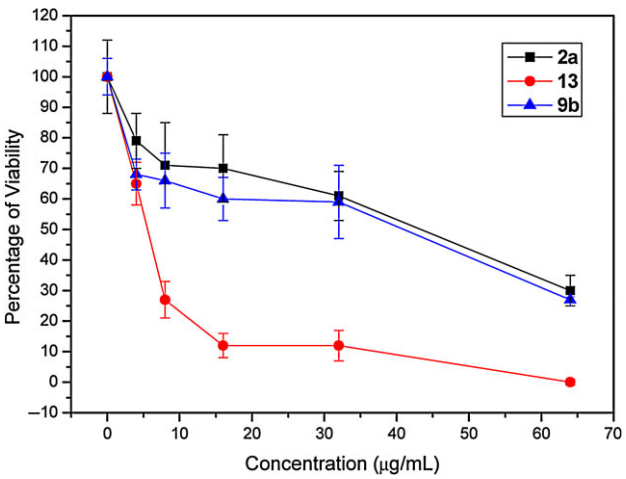

Figure 3. Viability of rat hepatocytes (HepG2) after treatment with compounds **2a**, **9b**, and **13**. Results are expressed as the percentage of controls (untreated hepatocytes).

their antimicrobial effect in order to obtain initial structures, which probably need further optimization to be considered a lead compound.

Conformational and electronic study

To better understand the above experimental results, we have carried out a conformational and electronic study on the most active compounds of this series to reveal the stereo-electronic characteristics of these molecules. We performed calculations for many compounds of this series but in order to keep the size of this paper, we only show here the results obtained for **2a**, **2c**, **9c**, and **13** because they are representatives of the whole series. The details of how this study was conducted are given as molecular modeling in Section 4.3.

Previously, we reported an exhaustive conformational and electronic study for compounds **2b**, **9a**, and **9b** [24]; therefore, taking advantage of this situation, we compared those results with the obtained here. As we expected, the conformational behavior obtained for compounds **2a** and **9c** is almost the same as that previously reported for **9b**, while the results obtained for **2c** are very similar to those reported for compound **9a**.

^{1}H and ^{13}C NMR spectra of non-symmetrically substituted compounds type **9** show two sets of signals, indicating that, in solution (DMSO-d_6), these compounds exist as two Ar–N=O rotamers α, β in equilibrium (Fig. 4). For compound **9b**, B3LYP/6-31G(d,p) calculation predicts that rotamer β possesses 0.04 kcal/mol above rotamer α and the energy barrier for the conformational interconversion is 27.6 kcal/mol. These results are in a complete agreement with our experimental results (see the spectrum shown in Supporting Information Fig. S1), with a ratio α/β around 57:43, as well as with the theoretical results recently reported by Prochazkova et al. [32]. Similar results were obtained for the rest of compounds type **9**. In the case of compounds type **10**, rotamers showed four sets of signals (see Supporting Information Fig. S2). DFT calculations predict the following energy gaps in kcal/mol for such rotamers of compound **10a**: α2 (0.0), α1 (0.06), β1 (0.26), and β2 (0.40), which is also in agreement with the ^{1}H and ^{13}C NMR data obtained (Fig. 5).

Conjugated nitrosamines belong to the same family as the enols of β-diketones and other conjugated systems with intramolecular hydrogen bonds. Therefore, the formation of intramolecular hydrogen bonds may be expected, and indeed, such interactions were found in the solid-state

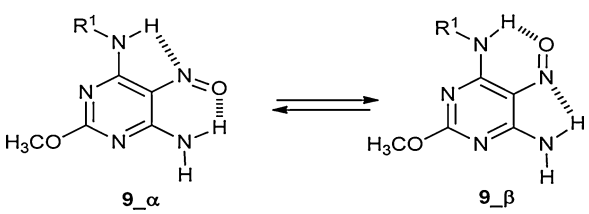

Figure 4. Structures of the rotamers α and β in equilibrium of compound **9**.

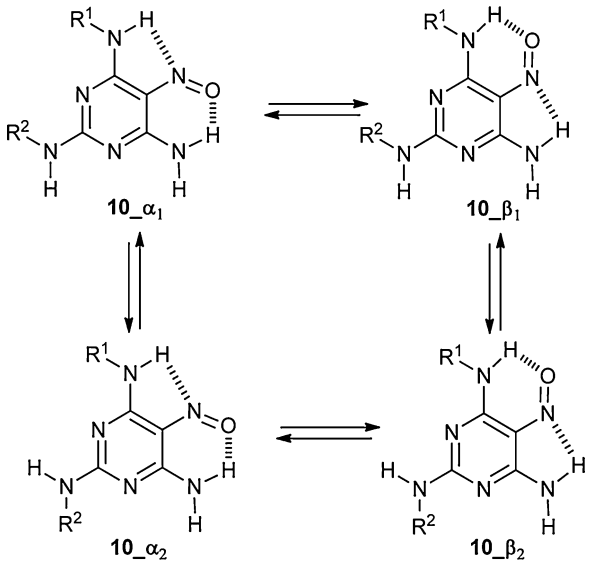

Figure 5. Structures of the rotamers α2, α1, β1, and β2 of compound **10a**.

structures of 3-amino-2-nitrosocyclohex-2-en-1-one [33], 5-amino-4-nitrosopyrazole [33], and 6-amino-5-nitrosopyrimidines [34–38]. Our results are in agreement with those of Prochazkova et al. reporting that a mixture of two forms with distinct hydrogen-bond patterns were found in the solutions of compounds with two hydrogen bond donors neighboring the nitroso group [32]. It is interesting to note that these authors also reported that the ratio of the two forms was significantly substituent-dependent, and the concentrations of the two forms can be found in a broad range.

Figure 6 shows a spatial view of the superimposed energetically preferred conformations obtained for the most active compounds (**2a–c**, **9a**,**b**,**e**, and **13**). The conformations of compounds **2b**, **9b**, and **13** previously reported [24] have been included here for comparison. From this figure, it is evident that all these compounds can adopt very similar conformations displaying the reactive groups in a similar spatial ordering. However, it is clear that not only the conformational aspects but also the electronic properties of these compounds are determinant for the antibacterial activities. Thus, the knowledge of the stereo-electronic attributes and properties of these nitrosopyrimidines will contribute significantly to the elucidation of the structural requirements to produce the antibacterial activity. Molecular electrostatic potentials (MEP) are of particular value because they allow the visualization and assessment of the capacity of a molecule to interact electrostatically with a putative binding site [39–41]. Thus, this methodology was used to evaluate the electronic distribution around molecular surface for compounds reported here.

Figure 7 gives the MEPs obtained for compounds **2a**, **9a**, **9e**, and **13**. The MEPs obtained for these compounds account

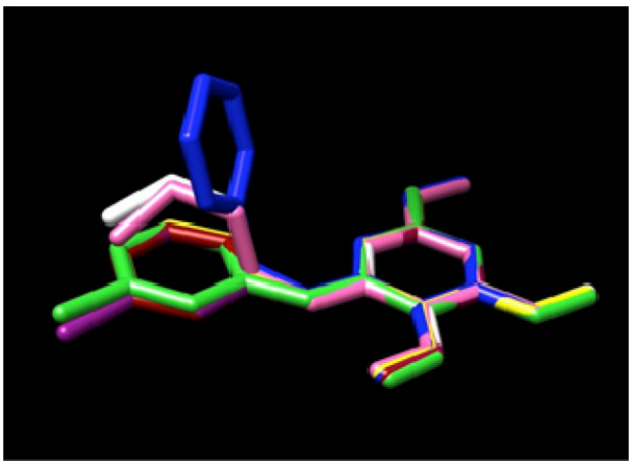

Figure 6. Spatial view of overlapping of the energetically preferred conformations obtained for compounds **2a** (yellow), **2b** (green), **2c** (white) **9a** (pink), **9b** (red), **9e** (violet), and **13** (blue).

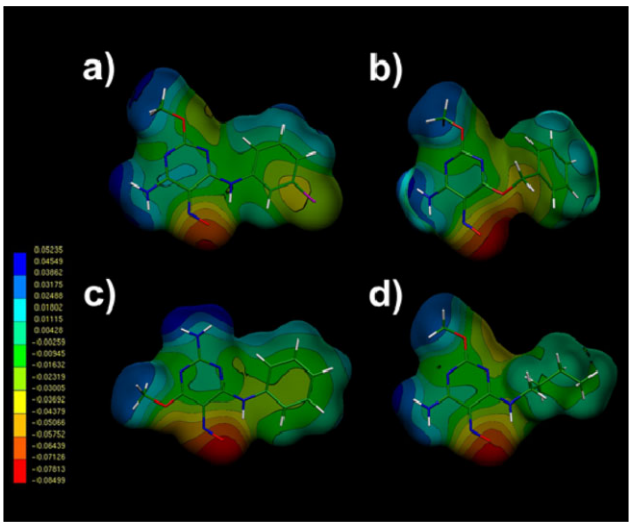

Figure 7. Electrostatic potential-encoded electron density surfaces of compounds **9c** (a), **13** (b), **2a** (c), and **9a** (d). The surfaces were generated with GAUSSIAN 03 using B3LYP/6-311++G(d,p) single point calculations. The coloring represents electrostatic potential with red indicating the strongest attraction to a positive point charge and blue indicating the strongest repulsion. The electrostatic potential is the energy of interaction of the positive point charge with the nuclei and electrons of a molecule. It provides a representative measure of overall molecular charge distribution. The color-code is shown at the left.

for the general characteristics of the electronic behavior for the active compounds. The general pattern is very similar for all these systems. The MEPs exhibit four characteristic regions: a clear minimum value (deep red zone with $V(r)_{min} \approx -0.0874$ el/au^3) in the vicinity of the NO group; two positive regions (deep blue zones with $V(r)_{max} \approx 0.054$ el/au^3) located near to the NH_2 and OCH_3 groups and an extended hydrophobic zone (deep and light green zone with an almost neutral potential $V(r)_{med} \approx -0.0022$ el/au^3) throughout the second ring (or the flexible side chain in the case of compound **9a**).

Table 3. log *S* and log *P* obtained for active compounds.

Comp.	log *S*	log *P*
2a	−4.12	2.53
2b	−4.85	3.09
2c	−3.44	1.81
9a	−3.44	1.81
9b	−4.12	2.53
9c	−3.71	2.04
9d	−3.92	2.29
9e	−4.85	3.09
13	−3.28	2.67

Finally, let us make some comments regarding pharmacokinetic properties of these compounds. Predictions of ADME, absorption, and distribution parameters and the calculated physicochemical properties (log *S* and log *P* in Table 3) for the active compounds, are within the typical ranges desired for a drug, as well as the fulfillment of Lipinski's rule, which permit us to consider these compounds as interesting starting structures for antibacterial activity. All these aspects serve to justify future research on new series of nitrosopyrimidines focused to the structural optimization that would lead to a substantial improvement of potency and spectrum in the antibacterial activity. Such research must be complemented with *in vivo* toxicity and efficacy evaluations and the establishing of the mechanism of action at molecular level.

Conclusions

The synthesis, *in vitro* evaluation and SAR studies of 35 nitrosopyrimidines and structurally related derivatives acting as antibacterial agents are reported. Several compounds showed a strong antibacterial activity, some of them with activities comparable to the reference compound used (cefotaxime). Unfortunately, some of these compounds also showed a significant acute toxicity, which severely limits its potential therapeutic use. However, other compounds showed strong antibacterial activity and relatively low acute toxicity like for example compounds **2a**, **2b**, **2c**, and **9b**. Thus, special attention might be given to these compounds since they not only showed the strongest antibacterial effects but at the same time they showed a relatively low acute toxicity, which converts these compounds like appropriate structures for the search of new antibacterial compounds. Our SAR study helped us to identify and understand the minimal structural requirements for the antibacterial action of these

compounds. Thus, we believe that our results may be helpful in the structural identification and understanding of the minimum structural requirements for the activity of these molecules and could provide a guide in the design of compounds with this biological activity.

Experimental

Chemistry

Melting points were determined on a Barstead Electrothermal 9100 apparatus and are uncorrected. IR spectra were recorded in KBr disks on Bruker TENSOR 27 spectrophotometer from Centro de Instrumentación Científico-Técnica (CICT) at Universidad de Jaén. ^{1}H and ^{13}C NMR spectra were recorded on a Bruker Avance 400 spectrophotometer (CICT) operating at 400 and 100 MHz, respectively, using $CDCl_3$ and DMSO-d_6 as solvents and tetramethylsilane as internal standard. Multiplicity of the carbons was assigned with DEPT and gHSQC experiments, although usual abbreviations according to off-resonance decoupling are used: (s) singlet, (d) doublet, (t) triplet, and (q) quartet. The same abbreviations were used for the multiplicity of signals in ^{1}H NMR and also: (m) multiplet and (bs) broad singlet. Coupling constants (*J*) are reported in Hertz. Mass spectra were run on a SHIMADZU-GCMS 2010-DI-2010 spectrometer (equipped with a direct inlet probe) operating at 70 eV. High-resolution mass spectra were run on a Waters Micromass AutoSpec-Ultima spectrometer (equipped with a direct inlet probe) operating at 70 eV. Silica gel aluminum plates (Merck 60 F254) were used for analytical TLC. The amines, aminoesters, 2-amino-4,6-dimethoxypyrimidine, and 4-amino-2,6-dimethoxypyrimidine were purchased from Aldrich, Fluka, and Acros (synthesis reagent grades) and were used without further purification. Solvents were purchased from the same vendors but purified according to the standard protocols. Compounds **1a–c**, **2–6**, **7b–c**, **8b–c**, **9b**, **9f**, **10e**, and **11–15** were synthesized using reported procedures [25–27].

*2-(2-Amino-6-cyclohexylmethoxy-5-nitrosopyrimidin-4-ylamino)acetic acid ethyl ester (**7a**)*

To a suspension of **1b** (174 mg, 0.50 mmol) in *t*-BuOH (5 mL), glycine ethyl ester hydrochloride (84 mg, 0.60 mmol) and Et_3N (61.3 mg, 0.60 mmol) were added. The mixture was stirred at 60°C and monotorized by TLC (silica, eluent: CH_2Cl_2/MeOH 9:1, v/v) until no starting material was visualized (4 h). Then, solvent was removed under reduced pressure and CH_2Cl_2 was added until solution. The organic solution was washed with water (3 × 15 mL) and dried on anhydrous sodium sulfate, and the solvent was removed under vacuum to offer compound **7a** as a blue solid (110 mg, 65%); m.p. 182–184°C (d), ^{1}H NMR (400 MHz, DMSO-d_6, 25°C) δ (ppm): 11.22 (t, $J = 6.0$ Hz, 1H, NH), 7.98 (bs, 1H, NH_2), 7.94 (bs, 1H, NH_2), 4.29 (d, $J = 6.6$ Hz, 2H, OCH_2), 4.16 (d, $J = 6.0$ Hz, 2H, NCH_2), 4.11 (q, $J = 7.1$ Hz, 2H, OCH_2), 1.82–1.64 (m, 7H, CH, $3CH_2$), 1.14–0.92 (m, 4H, $2CH_2$), 1.18 (t, $J = 7.1$ Hz, 3H, CH_3). ^{13}C NMR (100 MHz, DMSO-d_6) δ: 170.8 (s), 169.0 (s, CO), 163.3 (s), 150.0 (s), 138.8 (s), 71.7 (t), 60.7 (t), 41.2 (t), 36.7 (d), 29.1 (t), 25.9 (t), 25.1 (t), 14.0 (q). MS (EI, 70 eV): 338 (100), 337 (M^+, 63), 242 (22), 152 (40), 140 (30), 55 (68). HR-MS (EI): $C_{15}H_{23}N_5O_4$ requires 337.1750, found 337.1749.

*2-Amino-4-cyclohexylmethoxy-7,8-dihydro-5H-pteridin-6-one (**8a**)*

To a suspension of nitrosopyrimidine **7a** (168 mg, 0.50 mmol) in MeCN/H_2O (15 mL, 2:1, v/v) at 50°C, $Na_2S_2O_4$ (435 mg, 2.5 mmol) was slowly added until decoloration. Then, the mixture was evaporated to dryness, the residue was suspended in water and left at 4°C overnight. The precipitate was filtered, washed with water, and dried to give compound **8a** as a yellow solid (116 mg, 84%), m.p. 214–216°C (d). ^{1}H NMR (400 MHz, $CDCl_3$, 25°C) δ (ppm): 7.41 (bs, 1H, NH), 4.98 (bs, 1H, NH), 4.58 (bs, 2H, NH_2), 4.12 (s, 2H, NCH_2), 4.05 (d, $J = 6.6$ Hz, 2H, OCH_2), 1.78–1.67 (m, 6H, 2CH, $2CH_2$), 1.30–0.87 (m, 5H, CH, $2CH_2$). ^{13}C NMR (100 MHz, $CDCl_3$) δ: 162.1 (s, CO), 157.9 (s), 156.3 (s), 151.5 (s), 94.45 (s), 71.6 (t), 46.0 (t), 37.4 (d), 29.8 (t), 29.7 (t), 26.4 (t), 25.7 (t). IR (KBr): $\nu = 3344$, 3220, 2925, 2851, 1682, 1626, 1605, 1482 cm^{-1}. MS (EI, 70 eV): 277 (M^+, 22), 181 (100), 152 (50), 55 (25). HR-MS (EI): $C_{13}H_{19}N_5O_2$ requires 277.1539, found 277.1533.

*4-Amino-6-butylamino-2-methoxy-5-nitrosopyrimidine (**9a**)*

To a suspension of 4-amino-2,6-dimethoxy-5-nitrosopyrimidine **1c** (184 mg, 1.00 mmol) in dichloromethane (10 mL), *n*-butylamine (0.11 mL, 1.1 mmol) was added. The mixture was stirred at room temperature and monitored by TLC (silica, eluent: CH_2Cl_2/MeOH 9:1, v/v) until no starting material was visualized (20 h). Then, water (20 mL) was added and the organic phase was separated and dried on anhydrous sodium sulfate. The solid was removed and the solvent was eliminated, offering compound **9a** as a blue solid (183 mg, 81%), m.p. 139–141°C. ^{1}H NMR (400 MHz, $CDCl_3$, 25°C) δ (ppm): 11.51/7.95 (bs, 1H, NH), 10.62/7.68 (bs, 1H, NH_2), 6.51/6.31 (bs, 1H, NH_2), 3.99/3.97 (s, 3H, OCH_3), 3.81/3.53 (q, $J = 7.1$ Hz, 2H, NCH_2), 1.62 (m, 2H, CH_2); 1.42 (m, 2H, CH_2), 1.91 (m, 3H, CH_3). ^{13}C NMR (100 MHz, $CDCl_3$) δ: 168.2 (s), 168.1 (s), 150.2 (s), 137.8 (s), 55.3 (q), 39.6 (t), 31.0 (t), 20.1 (t), 13.7 (q). IR (KBr): $\nu = 3379$, 3191, 2957, 1643, 1593, 1342, 1275 cm^{-1}. MS (EI, 70 eV): 225 (M^+, 49), 208 (100), 182 (30), 154 (44). HR-MS (EI): $C_9H_{15}N_5O_2$ requires 225.1226, found 225.1223.

*4-Amino-6-(3-chlorophenyl)amino-2-methoxy-5-nitrosopyrimidine (**9c**)*

To a suspension of 4-amino-2,6-dimethoxy-5-nitrosopyrimidine **1c** (184 mg, 1.00 mmol) in water (10 mL), 3-chloroaniline (0.21 mL, 2.0 mmol) was added. The mixture was stirred at 80°C and monitored by TLC (silica, eluent: CH_2Cl_2/MeOH 9:1, v/v) until no starting material was visualized (5 h). Then, the precipitate was filtered, washed, and finally, dried in a vacuum desiccator over potassium hydroxide pellets offering compound **9c** as a green solid (182 mg, 65%), m.p. 203–205°C

(d). ^{1}H NMR (400 MHz, DMSO-d_6, 25°C) δ (ppm): 13.41/10.32 (s, 1H, NH), 11.09/9.19 (bs, 1H, NH_2), 8.71/8.39 (bs, 1H, NH_2), 8.13–8.07 (m, 1H, Ph), 7.89–7.60 (m, 1H, Ph), 7.63–7.37 (m, 1H, Ph), 7.26–7.19 (m, 1H, Ph), 3.92/3.91 (s, 3H, OCH_3). ^{13}C NMR (100 MHz, DMSO-d_6) δ: 167.6/167.0 (s), 163.5 (s), 149.5/146.8 (s), 139.8/138.6 (s), 138.2/137.5 (s), 133.1/132.6 (s), 130.5/130.0 (d), 124.9/123.8 (d), 123.0/122.4 (d), 121.6/121.3 (d), 55.0 (q). IR (KBr): ν = 3245, 3076, 2958, 1612, 1554, 1473, 1329, 1267, 1046 cm^{-1}. MS (EI, 70 eV): 279 (M^+, 56), 262 (100), 245 (39), 192 (19), 111 (37), 58 (62). HR-MS (EI): $C_{11}H_{10}N_5O_2$ requires 279.0523, found 279.0518.

*4-Amino-6-benzylamino-2-methoxy-5-nitrosopyrimidine (**9d**)*

To a suspension of 4-amino-2,6-dimethoxy-5-nitrosopyrimidine **1c** (184 mg, 1.00 mmol) in acetonitrile (10 mL), benzylamine (0.13 mL, 1.2 mmol) was added. The mixture was stirred at room temperature and monitored by TLC (silica, eluent: CH_2Cl_2/MeOH 9:1, v/v) until no starting material was visualized (20 h). Then, water (20 mL) was added and the solid in suspension was filtered, washed, and finally, dried in a vacuum desiccator over potassium hydroxide pellets offering compound **9d** as a blue solid (233 mg, 90%), m.p. 218–220°C. ^{1}H NMR (400 MHz, DMSO-d_6, 25°C) δ (ppm): 11.72/10.00 (t, J = 6.0, 6.6 Hz; 1H, NH), 10.34/8.94 (bs, 1H, NH_2), 8.52/8.11 (bs, 1H, NH_2), 7.42–7.24 (m, 5H, Ph), 4.71/4.62 (d, J = 6.6, 6.0 Hz; 2H, NCH_2), 3.84/3.83 (s, 3H, OCH_3). ^{13}C NMR (100 MHz, DMSO-d_6) δ: 167.8/167.5 (s), 164.7 (s), 149.9/149.2 (s), 139.1 (s), 138.1, 138.0 (s), 128.5/128.3 (d), 127.7/127.5 (d), 127.2/126.9 (d), 54.8/54.7 (q), 43.7/42.7 (t). IR (KBr): ν = 3356, 3203, 2952, 1642, 1593, 1528, 1456, 1339, 1288 cm^{-1}. MS (EI, 70 eV): 259 (M^+, 12), 242 (100), 210 (19), 154 (32), 105 (16), 91 (60), 65 (27). HR-MS (EI): $C_{12}H_{13}N_5O_2$ requires 259.1069, found 259.1067.

*4-Amino-6-(3,4-dimethoxybenzyl)methylamino-2-methoxy-5-nitrosopyrimidine (**9e**)*

To a suspension of 4-amino-2,6-dimethoxy-5-nitrosopyrimidine **1c** (184 mg, 1.00 mmol) in acetonitrile (10 mL), 3,4-dimethoxybenzylamine (0.19 mL, 1.2 mmol) was added. The mixture was stirred at room temperature and monitored by TLC (silica, eluent: CH_2Cl_2/MeOH 9:1, v/v) until no starting material was visualized (20 h). Then, water (20 mL) was added and the solid in suspension was filtered, washed, and finally, dried in a vacuum desiccator over potassium hydroxide pellets offering compound **9e** as a blue solid (232 mg, 73%), m.p. 195–197°C. ^{1}H NMR (400 MHz, $CDCl_3$, 25°C) δ (ppm): 11.58/8.12 (bs, 1H, NH), 10.44/7.58 (bs, 1H, NH_2), 6.95–6.81 (m, 3H, Ph), 5.90/5.74 (bs, 1H, NH_2), 4.78/4.63 (d, J = 5.8 Hz; 2H, NCH_2), 4.00/3.99 (s, 3H, OCH_3), 3.87/3.86 (s, 6H, 2OCH_3). ^{13}C NMR (100 MHz, $CDCl_3$) δ: 168.2 (s), 165.2 (s), 149.7 (s), 149.3 (s), 148.9/148.8 (s), 138.4/137.9 (s), 129.6/129.1 (d), 120.5/120.3 (d), 111.5/111.3 (d), 56.0 (q), 55.4 (q), 45.0, 43.7 (t). IR (KBr): ν = 3405, 3305, 2954, 1632, 1598, 1520, 1465, 1370, 1274 cm^{-1}. MS (EI, 70 eV): 319 (M^+, 8), 302 (100), 286 (37), 151 (30). HR-MS (EI): $C_{14}H_{17}N_5O_4$ requires 319.1281, found 319.1279.

*4-Amino-6-butylamino-2-(2-hydroxyethylamino)-5-nitrosopyrimidine (**10a**)*

To a suspension of 5-nitrosopyrimidine **9a** (225 mg, 1.00 mmol) in methanol (10 mL), 2-aminoethanol (0.12 mL, 2.0 mmol) was added. The mixture was stirred, refluxed, and monitored by TLC (silica, eluent: CH_2Cl_2/MeOH 9:1, v/v) until no starting material was visualized (12 h). After cooling, the precipitate was filtered, washed, and finally, dried in a vacuum desiccator over potassium hydroxide pellets offering compound **10a** as a pink solid (182 mg, 72%), m.p. 184–186°C. ^{1}H NMR (400 MHz, DMSO-d_6, 25°C) δ (ppm): 11.65/11.39/10.61/10.28 (t, J = 5.5, 5.6 Hz, 1H, NH), 8.82/8.56/7.95/7.66 (t, J = 6.0, 5.8 Hz, 1H, NH), 8.23/7.66/7.51 (bs, 1H, NH_2), 8.02/7.66/7.26 (bs, 1H, NH_2), 4.72 (bs, 1H, OH), 3.86 (m, 2H, OCH_2), 3.52–3.37 (m, 4H, NCH_2), 1.64–1.44 (m, 2H, CH_2); 1.39–1.26 (m, 2H, CH_2), 1.91 (m, 3H, CH_3). ^{13}C NMR (100 MHz, DMSO-d_6) δ: 165.8/165.2 (s), 163.0/162.8/162.3 (s), 150.9/150.8/150.5/150.2 (s), 137.3/136.7 (s), 59.9/59.8 (t), 43.7/43.5 (t), 39.6/38.2 (t), 31.0/30.6 (t), 19.8/19.7 (t), 13.8/13.6 (q). IR (KBr): ν = 3308, 2964, 1665, 1592, 1360, 1198, 1048 cm^{-1}. MS (EI, 70 eV): 255 (MH^+, 100), 237 (58), 183 (31), 43 (27). HR-MS (EI): $C_{10}H_8N_6O_2$ requires 254.1491, found 254.1494.

*4-Amino-6-phenylamino-2-(2-hydroxyethylamino)-5-nitrosopyrimidine (**10b**)*

To a suspension of 5-nitrosopyrimidine **9d** (123 mg, 0.50 mmol) in methanol (5 mL), 2-aminoethanol (0.06 mL, 1.0 mmol) was added. The mixture was stirred, refluxed, and monitored by TLC (silica, eluent: CH_2Cl_2/MeOH 9:1, v/v) until no starting material was visualized (12 h). After cooling, the precipitate was filtered, washed, and finally, dried in a vacuum desiccator over potassium hydroxide pellets offering compound **10b** as a pink solid (82 mg, 60%), m.p. 208–210°C. ^{1}H NMR (400 MHz, DMSO-d_6, 25°C) δ (ppm): 14.07/13.72/10.42/10.19 (bs, 1H, NH), 10.57/10.23/8.46/8.25 (bs, 1H, NH_2), 8.18–8.04 (bs, 1H, NH), 8.01/7.98/7.70/7.51 (bs, 1H, NH_2), 7.95–7.77 (m, 2H, Ph), 7.39–7.29 (m, 2H, Ph), 7.16–7.05 (m, 1H, Ph), 4.78–4.72 (m, 1H, OH), 3.58–3.50 (m, 2H, OCH_2), 3.48–3.39 (m, 2H, NCH_2). ^{13}C NMR (100 MHz, DMSO-d_6) δ: 165.7/165.0 (s), 163.0/162.9/162.5/160.7 (s), 150.7/150.6/147.8/147.5 (s), 139.0/138.7/138.0/137.2 (s), 137.6/136.2 (s), 129.0/128.9/128.4 (d), 124.5/124.2/123.55/123.31 (d), 122.4/122.3/122.1/122.0 (d), 59.7/59.6 (t), 44.0/43.7 (t). IR (KBr): ν = 3242, 2953, 1613, 1587, 1558, 1340, 1053 cm^{-1}. MS (EI, 70 eV): 274 (M^+, 100), 257 (63), 239 (16), 212 (47), 144 (16), 77 (40). HR-MS (EI): $C_{12}H_{14}N_6O_2$ requires 274.1178, found 274.1177.

*4-Amino-6-(3,4-dimethoxyphenyl)methylamino-2-(2-hydroxyethylamino)-5-nitrosopyrimidine (**10c**)*

To a suspension of 5-nitroso-pyrimidine **9c** (159 mg, 0.50 mmol) in methanol (5 mL), 2-aminoethanol (0.06 mL, 1.0 mmol) was added. The mixture was stirred, refluxed, and monitored by TLC (silica, eluent: CH_2Cl_2/MeOH 9:1, v/v) until no starting material was visualized (12 h). After cooling, the precipitate was filtered, washed, and finally, dried in a vacuum desiccator over potassium hydroxide pellets offering

title compound as a pink solid (104 mg, 60%), m.p. 200–202°C (d). ^{1}H NMR (400 MHz, DMSO-d_6, 25°C) δ (ppm): 11.84, 11.52, 9.31, 9.00 (t, $J = 5.5$, 5.6 Hz, 1H, NH), 10.54, 10.22, 8.25, 8.02 (bs, 1H, NH_2), 8.01, 7.55, 7.53, 7.27 (bs, 1H, NH_2), 7.70 (bs, 1H, NH), 7.04–6.84 (m, 3H, Ph); 4.72–4.65 (m, 1H, OH), 4.65–4.45 (m, NCH_2), 3.70 (s, 6H, $2OCH_3$), 3.55–3.44 (m, 2H, OCH_2), 3.41–3.34 (m, 2H, NCH_2). ^{13}C NMR (100 MHz, DMSO-d_6) δ: 165.8, 165.2, 163.0, 162.8, 162.7, 162.6, 150.8, 150.0, 149.7, 148.7, 148.6, 148.0, 147.8, 137.4, 136.8, 136.7, 132.1, 132.0, 130.8, 130.6 (s), 120.1 119.9 (d), 112.0, 111.9 (d), 111.8 (d), 59.7 (t), 55.4 (q), 43.6 (t), 42.1 (t). IR (KBr): $\nu = 3510$, 3341, 3168, 2938, 1648, 1602, 1544, 1321, 1255, 1168, 1032 cm^{-1}. MS (EI, 70 eV): 348 (M^+, 3), 330 (63), 299 (98), 283 (39), 183 (41), 151 (100), 120 (42), 107 (47), 43 (84). HR-MS (EI): $C_{15}H_{20}N_6O_4$ requires 348.1546, found 348.1546.

*4-Amino-2,6-bis(2-hydroxyethylamino)-5-nitrosopyrimidine (**10d**)*

To a suspension of 4-amino-2,6-dimethoxy-5-nitrosopyrimidine **1c** (184 mg, 1.00 mmol) in methanol (10 mL), 2-aminoethanol (0.14 mL, 2.4 mmol) was added. The mixture was stirred, refluxed, and monitored by TLC (silica, eluent: CH_2Cl_2/MeOH 9:1, v/v) until no starting material was visualized (12 h). After cooling, the precipitate was filtered, washed, and finally, dried in a vacuum desiccator over potassium hydroxide pellets offering title compound as a pink solid (187 mg, 77%), m.p. 210–212°C (d). ^{1}H NMR (400 MHz, DMSO-d_6, 25°C) δ (ppm): 11.64/11.37/8.63/8.42 (t, $J = 5.5$, 5.6 Hz, 1H, NH), 10.57/10.24/8.24/8.02 (bs, 1H, NH_2), 7.64 (bs, 1H, NH), 8.01/7.71/7.51/7.25 (bs, 1H, NH_2), 4.88 (bs, 1H, OH), 4.72 (bs, 1H, OH), 3.62–3.17 (m, 8H, $2OCH_2 + 2NCH_2$). ^{13}C NMR (100 MHz, DMSO-d_6) δ: 165.9, 165.3 (s), 163.0, 162.8 (s), 150.9, 150.8, 150.4, 150.2 (s), 137.3, 136.8 (s), 59.9, 59.8, 59.6 (t), 59.5, 59.2, 59.1 (t), 43.7, 43.5, 42.8, 42.6 (t), 41.3, 41.4 (t). IR (KBr): $\nu = 3370$, 3324, 2940, 1651, 1602, 1560, 1382, 1192, 1058 cm^{-1}. MS (EI, 70 eV): 242 (M^+, 100), 225 (53), 211 (52), 195 (79), 183 (73), 177 (39), 68 (57), 43 (98). HR-MS (EI): $C_8H_{14}N_6O_3$ requires 242.1127, found 242.1123.

*2-{2-[(4-Amino-6-{[2-(2-hydroxyethoxy)ethyl]amino}-5-nitrosopyrimidin-2-yl)amino]ethoxy}ethanol (**10e**)*

To a suspension of 4-amino-2,6-dimethoxy-5-nitrosopyrimidine **1c** (184 mg, 1.00 mmol) in methanol (10 mL), 2-(2-aminoethoxy)ethanol (0.25 mL, 2.4 mmol) was added. The mixture was stirred, refluxed, and monitored by TLC (silica, eluent: CH_2Cl_2/MeOH 9:1, v/v) until no starting material was visualized (24 h). After cooling, solution was concentrated in vacuum to remove methanol and then, acetonitrile was added. The precipitate was filtered, washed, and finally, dried in a vacuum dessiccator over potassium hydroxide pellets offering title compound as a pink solid (230 mg, 70%), m.p. 144–146°C (d). ^{1}H NMR (400 MHz, DMSO-d_6, 25°C) δ (ppm): 11.59, 11.33, 8.71, 8.47 (bs, 1H, NH), 10.53, 10.21, 8.26, 8.06 (bs, 1H, NH_2), 7.73 (bs, 1H, NH), 8.04, 7.751, 7.54, 7.26 (bs, 1H, NH_2), 4.61 (bs, 1H, OH), 4.59 (bs, 1H, OH), 4.79–3.38 (m, 16H, $4OCH_2 + 4NCH_2$). ^{13}C NMR (100 MHz, DMSO-d_6) δ: 165.7, 165.2 (s), 162.8, 162.6 (s), 150.7, 150.5, 150.2, 149.9 (s), 137.3, 136.7 (s), 72.7 (t), 72.6 (t), 69.4, 69.3 (t), 68.9, 68.9 (t), 60.7 (t), 41.2, 41.1 (t), 39.1, 39.0 (t). IR (KBr): $\nu = 3368$, 3323, 2938, 1580, 1555, 1384, 1175, 1121 cm^{-1}. MS (EI, 70 eV): 330 (M^+, 4), 313 (4), 227 (7), 177 (10), 84 (13), 66 (21), 45 (100). HR-MS (EI): $C_{12}H_{22}N_6O_5$ requires 330.1652, found 330.1653.

Biological screenings

Microorganisms

The following strains were used: *S. aureus* methicillin-sensitive ATCC 29213, *S. aureus* methicillin-resistant ATCC 43300, *E. coli* ATCC 25922, *E. coli* LM1 (LM: Laboratorio de Microbiología, Facultad de Ciencias Médicas, Universidad Nacional de Cuyo, Mendoza, Argentina), *E. coli* LM2, *P. aeruginosa* ATCC 27853, *Y. enterocolitica* PI (PI: Pasteur Institute), *S. enteritidis* MI (MI: Malbrán Institute), and *Salmonella* sp. LM.

Antibacterial activity

The minimal inhibitory concentration (MIC) values were determined using the microbroth dilution method according to the protocols of the Clinical and Laboratory Standards Institute (CLSI, 20012) [42].

All tests were performed in Mueller-Hinton broth (MHB), and cultures of each strain were prepared overnight. Microorganisms suspensions were adjusted in a spectrophotometer with sterile physiological solution to give a final organism density of 0.5 McFarland scale ($1–5 \times 10^5$ CFU/mL). Stock solutions of peptides in DMSO were diluted to give serial twofold dilutions that were added to each medium to obtain final concentrations ranging from 0.25 to 50 μg/mL. The final concentration of DMSO in the assay did not exceed 1%. The Cefotaxime® Argentia Pharmaceutica antimicrobial agent was included in the assays as a positive control. The plates were incubated for 24 h at 37°C. The MIC was defined as the lowest peptide concentration showing no visible bacterial growth after incubation time. Tests were done in triplicate.

Acute toxicity test

Toxic effect of compounds was evaluated using a toxicity test on fish. The static technique recommended by the US Fish and Wildlife Service Columbia National Fisheries Research Laboratory [43] was modified in order to use lower amounts of tested compounds [44]. Fish of the specie *Poecilia reticulata* were born and grown in our laboratory until they reached a size of 0.7–1 cm (15 days old). In the toxicity test, 10 specimens were exposed to each of the concentration tested per drug in 2 L wide-mouthed jars containing the test solutions. Aqueous stock solutions of pure compounds diluted in DMSO were prepared and added to test chambers to get the final concentrations. The test began upon initial exposure to the peptides and continued for 96 h. The number of dead organisms in each test chamber was recorded and the dead organisms were removed every 24 h; general observations on the conditions of tested organisms were also recorded at this time; however the percentage of mortality was recorded at 96 h. Each experience was performed two times with three

replicates each. We chose this technique because it is fast, economic, and easy to reproduce. This assay has been previously used by our group to test the toxicity of synthetic and natural compounds [16, 44]. The species *P. reticulata* has been previously used in acute toxicity test [45].

Culture of HepG2 cells

HepG2 cells were cultured in Ham's F-12/Leibovitz L-15 (1:1 v/v) supplemented with 7% newborn calf serum, 50 U penicillin/mL, and 50 μg streptomycin/mL. For sub-culturing purposes, cells were detached by treatment with 0.25% trypsin/0.02% EDTA at 37°C. Cultures were used at 75% confluency.

MTT assay

Cytotoxicity effects were measured by using the MTT (tetrazoliun salt) reduction assay after 24 h of exposure to different concentrations of the compound (g/mL). The stock solution of the extract or compounds was prepared at a concentration of 1 mg/mL in culture medium and conveniently diluted in culture medium to obtain the final desired concentrations. Control cells (only medium-treated cells) were included in all experiments.

The MTT assay was performed according to the method of Jover et al. [46] Briefly, the medium was removed after exposure and cultures were washed with PBS. Then, 100 μL/well MTT reagent (5 mg/mL in medium) was added to each well and plates were placed in the incubator for a further 3 h. The corresponding supernatants were discarded and cells were washed again. The dye was extracted with DMSO and optical density was read at 490 nm on a microplate reader. The percentage of inhibition (%) of the succinic dehydrogenase reduction of MTT was calculated in relation to control cells in each experimental series (control cells were assumed to have 100% viability).

Molecular modeling

All the calculations reported here were performed using the GAUSSIAN 09 program [47]. Critical points (low-energy conformations and transition state structures) were optimized at DFT level of theory. Density functional theory (DFT) with the Becke-3-Lee-Yang-Parr (RB3LYP) functional [48–50] and 6-31G(d) basis set calculations were used in the optimization jobs of minimum obtained from potential energy surface (PES). An extensive search to localize the critical points on the PEHSs was carried out first by using starting geometries suggested by GASCOS algorithm [51]. These input files were used to obtain the low-energy conformations and TS structures using RHF/6-31G(d) calculations. Vibrational frequencies for the optimized structures were computed to evaluate the zero-point energies (ZPE) as well as to confirm the nature of the singular points along the PES. The stationary points have been identified as a minimum with no imaginary frequencies, or as a first-order transition state characterized by the existence of only one imaginary frequency in the normal mode coordinate analysis. Transition state structures were located until the Hessian matrix had only one imaginary eigenvalue, and the transition states were also confirmed by animating the negative eigenvectors coordinate with a visualization program and internal reaction coordinate (IRC) calculations [52, 53]. HF/6-31G(d) IRC calculations were performed on the transition state structures to check that the TSs structures lead to the initial conformer and to the final conformation (forward and reverse directions of the conformational interconversion path). IRC calculations steps 6 points in Cartesian coordinates in the forward direction and 6 points in the reverse direction, in step of 03 amu$^{1/2}$ Bohr along the path were carried out.

The electronic study of nitrosopyrimidines was carried out using MEPs [54]. The low energy conformations were obtained for these compounds from our conformational search. Subsequently, single point calculations were carried out. Thus, these MEPs were calculated using B3LYP/6-311++G(d,p) wave functions and MEPs graphical presentations were created using the MOLEKEL program [55]. The overlapping graphics images were produced using the UCSF Chimera package [56].

R.D.E. acknowledges ANPCyT, PICT 2010-1832. Grants from Universidad Nacional de San Luis (UNSL), partially supported this work. Authors thank "Centro de Instrumentación Científico Técnica" and the staff for data collection. The financial support from the Consejería de Economía, Innovación y Ciencia (Junta de Andalucía, Spain), the Universidad de Jaén and Ministerio de Ciencia e Innovación (project reference SAF2008-04685-C02-02) is thanked. R.D.E., G.E.F., and S.A.A. are members of the Consejo Nacional de Investigaciones Científicas y Técnicas (CONICET-Argentina) staff. B.L. is a fellowship of CONICET and thanks CICITCA-UNSJ for a grant.

The authors have declared no conflict of interest.

References

[1] B. A. Rogers, Z. Aminzadeh, Y. Hayashi, D. L. Paterson, *Clin. Infect. Dis.* **2011**, *53*, 49–56.
[2] M. Delgado-Valverde, J. Sojo-Dorado, Á. Pascual, J. Rodríguez-Baño, *Ther. Adv. Infect. Dis.* **2013**, *1*, 49–69.
[3] D. Talon, *J. Hosp. Infect.* **1999**, *43*, 13–17.
[4] A. Persidis, *Nat. Biotechnol.* **1999**, *17*, 1141–1142.
[5] A. Polak, *Mycoses* **1999**, *42*, 355–370.
[6] a) J. Bartroli, E. Turmo, M. Algueró, E. Boncompte, M. Vericat, L. Conte, J. Ramis, M. Merlos, J. García-Rafanell, J. Forn, *J. Med. Chem.* **1998**, *41*, 1855–1868; b) J. Bartroli, E. Turmo, M. Algueró, E. Boncompte, M. Vericat, L. Conte, J. Ramis, M. Merlos, J. García-Rafanell, *J. Med. Chem.* **1998**, *41*, 1869–1882.
[7] T. J. Walsh, A. Groll, J. Hiemenz, R. Fleming, E. Roilides, E. Anaissie, *Clin. Microbiol. Infect.* **2004**, *10*, 48–66.
[8] M. F. Masman, A. M. Rodriguez, L. Svetaz, S. A. Zacchino, C. Somlai, I. G. Csizmadia, B. Penke, R. D. Enriz, *Bioorg. Med. Chem.* **2006**, *14*, 7604–7614.

[9] M. F. Masman, A. M. Rodriguez, M. Raimondi, S. A. Zacchino, P. G. Luiten, C. Somlai, T. Kortvelyesi, B. Penke, R. D. Enriz, *Eur. J. Med. Chem.* **2009**, *44*, 212–228.
[10] F. Garibotto, A. D. Garro, C. Somlai, M. F. Masman, P. Lutien, S. A. Zacchino, A. M. Rodriguez, B. Penke, R. D. Enriz, *Bioorg. Med. Chem.* **2010**, *18*, 158–170.
[11] M. S. Olivella, A. M. Rodriguez, C. Somlai, B. Penke, V. Farkas, A. Perczel, R. D. Enriz, *Bioorg. Med. Chem. Lett.* **2010**, *20*, 4808–4811.
[12] F. M. Garibotto, A. D. Garro, A. M. Rodríguez, M. Raimondi, S. A. Zacchino, A. Perczel, C. Somlai, B. Penke, R. D. Enriz, *Eur. J. Med. Chem.* **2011**, *46*, 370–377.
[13] A. D. Garro, M. S. Olivella, J. A. Bombasaro, B. Lima, A. Tapia, G. Feresin, A. Perczel, C. Somlai, B. Penke, J. López Cascales, A. M. Rodríguez, R. D. Enriz, *Chem. Biol. Drug Des.* **2013**, *82*, 167–177.
[14] S. Zacchino, S. A. Lopez, G. Pezzenati, R. Furlan, C. Santecchia, L. Muñoz, F. Giannini, A. M. Rodriguez, R. D. Enriz, *J. Nat. Prod.* **1999**, *63*, 1353–1357.
[15] R. R. Kurdelas, B. Lima, A. Tapia, G. Feresin, M. Gonzalez Sierra, M. V. Rodríguez, S. Zacchino, R. D. Enriz, M. L. Freile, *Molecules* **2010**, *15*, 4898–4907.
[16] M. L. Freile, F. Giannini, G. Pucci, A. Sturniollo, L. R. Dodero, O. Pucci, V. Balzareti, R. D. Enriz, *Fitoterapia* **2003**, *74*, 702–705.
[17] M. Derita, I. Montenegro, F. Garibotto, R. D. Enriz, M. C. Fritis, S. A. Zacchino, *Molecules* **2013**, *18*, 2029–2050.
[18] M. Derita, E. Del Olmo, B. Barboza, A. E. García-Cadenas, J. L. López-Pérez, S. Andújar, R. D. Enriz, S. A. Zacchino, A. S. Feliciano, *Molecules* **2013**, *18*, 3479–3501.
[19] L. J. Gutierrez, M. L. Mascotti, M. B. Kurina-Sanz, C. Pungitore, R. D. Enriz, F. A. Giannini, *Nat. Prod. Commun.* **2012**, *7*, 1639–1644.
[20] M. Sortino, F. Garibotto, V. Cechinel Filho, M. Gupta, R. Enriz, S. Zacchino, *Bioorg. Med. Chem.* **2011**, *19*, 2823–2833.
[21] V. V. Kouznetsov, L. Y. Vargas Mendes, M. Sortino, Y. Vasquez, M. P. Gupta, M. Freile, R. D. Enriz, S. Zacchino, *Bioorg. Med. Chem.* **2008**, *16*, 794–809.
[22] M. A. Sortino, P. Delgado, S. F. Juarez, J. Quiroga, R. Abonía, B. Insuasty, M. Nogueras, L. Rodero, F. Garibotto, R. D. Enriz, S. A. Zacchino, *Bioorg. Med. Chem.* **2007**, *15*, 484–494.
[23] L. Karolyhazy, M. L. Freile, M. Anwair Gy Beke, F. Giannini, M. Sortino, J. C. Ribas, S. Zacchino, P. Matyus, R. D. Enriz, *Arzneim.- Forsch./-Drug Res.* **2003**, *53*, 738–743.
[24] M. Olivella, A. Marchal, M. Nogueras, A. Sánchez, M. Melguizo, M. Raimondi, S. Zacchino, F. Giannin, J. Cobo, R. D. Enriz, *Bioorg. Med. Chem.* **2012**, *20*, 6109–6122.
[25] A. Marchal, M. Nogueras, A. Sánchez, J. N. Low, L. Naesens, E. De Clercq, M. Melguizo, *Eur. J. Org. Chem.* **2010**, *2*, 3823–3830.
[26] J. Cobo, M. Nogueras, J. N. Low, R. Rodríguez, *Tetrahedron Lett.* **2008**, *49*, 7271–7273.
[27] A. Marchal, M. Melguizo, M. Nogueras, A. Sánchez, J. N. Low, *Synlett* **2002**, *20*, 255–258.
[28] J. Quiroga, J. Trilleras, B. Insuasty, R. Abonía, M. Nogueras, A. Marchal, J. Cobo, *Tetrahedron Lett.* **2008**, *49*, 3257–3259.
[29] C. Glidewell, J. N. Low, A. Marchal, A. Quesada, *Acta Crystallogr. Sect. C* **2003**, *59*, 454–460.
[30] E. R. Correché, S. A. Andujar, R. R. Kurdelas, M. J. Gómez Lechón, M. L. Freile, R. D. Enriz, *Bioorg. Med. Chem.* **2008**, *16*, 3641–3651.
[31] C. Somlai, E. Correche, M. Olivella, L. Tolos, M. J. Gomez Lechon, G. Dombi, G. K. To'th, B. Penke, R. D. Enriz, *Bioorg. Med. Chem. Lett.* **2012**, *22*, 4233–4237.
[32] E. Prochazkova, L. Cechova, Z. Janeba, M. Dracˇínsky, *J. Org. Chem.* **2013**, *78*, 10121–10133.
[33] P. Gilli, V. Bertolasi, V. Ferretti, G. J. Gilli, *Am. Chem. Soc.* **2000**, *122*, 10405–10417.
[34] M. H. Holschbach, D. Sanz, R. M. Claramunt, L. Infantes, S. Motherwell, P. R. Raithby, M. L. Jimeno, D. Herrero, I. Alkorta, N. Jagerovic, J. Elguero, *J. Org. Chem.* **2003**, *68*, 8831–8837.
[35] A. Marchal, M. Nogueras, A. Sanchez, J. N. Low, L. Naesens, E. De Clercq, M. Melguizo, *Eur. J. Org. Chem.* **2010**, *20*, 3823–3830.
[36] G. Urbelis, I. Susvilo, S. Tumkevicius, *J. Mol. Model.* **2007**, *13*, 219–224.
[37] I. Susvilo, A. Brukstus, S. Tumkevicius, *Tetrahedron Lett.* **2005**, *46*, 1841–1844.
[38] M. Melguizo, A. Quesada, J. N. Low, C. Glidewell, *Acta Crystallogr, Sect. B* **2003**, *59*, 263–276.
[39] P. Politzer, D. G. Truhlar, *Chemical Applications of Atomic and Molecular Electrostatic Potentials*, Plenum Press, New York **1981**, p. 1.
[40] P. A. Carrupt, N. El Tayar, A. Karlén, B. Festa, *Methods Enzymol.* **1991**, *202*, 638–650.
[41] P. Greeling, W. Langenaeker, F. De Proft, A. Baeten, in *Molecular Electrostatic Potentials: Concepts and Applications. Theoretical and Computational Chemistry*, Vol. *3*, Elsevier Science B.V., Amsterdam **1996**, pp. 587–617.
[42] CLSI, *Performance standards for Antimicrobial Susceptibility Testing*, Twenty-Second Informational Supplement. CLSI document M100-S22, Clinical and Laboratory Standards Institute, Wayne, PA **2012**.
[43] W. W. Johnsosn, M. T. Finley, *Handbook of Acute Toxicity of Chemicals to Fish and Aquatic Invertebrates*, United States Department of the Interior Fish and Wildlife Service, Washington, DC **1980**, p. 1.
[44] F. Bisogno, L. Mascotti, C. Sanchez, F. Garibotto, F. Giannini, M. Kurina, R. D. Enriz, *J. Agric. Food Chem.* **2007**, *55*, 10635–10640.
[45] W. Slooff, D. De Zwart, J. Van de Kerkhoff, *Aquat. Toxicol.* **1983**, *4*, 189–198.
[46] R. Jover, X. Ponsoda, J. V. Castell, M. J. Gómez-Lechón, *Toxicol. In Vitro* **1992**, *6*, 47–52.
[47] M. J. Frisch, G. W. Trucks, H. B. Schlegel, G. E. Scuseria, M. A. Robb, J. R. Cheeseman, G. Scalmani, V. Barone,

B. Mennucci, G. A. Petersson, H. Nakatsuji, M. Caricato, X. Li, H. P. Hratchian, A. F. Izmaylov, J. Bloino, G. Zheng, J. L. Sonnenberg, M. Hada, M. Ehara, K. Toyota, R. Fukuda, J. Hasegawa, M. Ishida, T. Nakajima, Y. Honda, O. Kitao, H. Nakai, T. Vreven, J. A. Montgomery, Jr., J. E. Peralta, F. Ogliaro, M. Bearpark, J. J. Heyd, E. Brothers, K. N. Kudin, V. N. Staroverov, R. Kobayashi, J. Normand, K. Raghavachari, A. Rendell, J. C. Burant, S. S. Iyengar, J. Tomasi, M. Cossi, N. Rega, J. M. Millam, M. Klene, J. E. Knox, J. B. Cross, V. Bakken, C. Adamo, J. Jaramillo, R. Gomperts, R. E. Stratmann, O. Yazyev, A. J. Austin, R. Cammi, C. Pomelli, J. W. Ochterski, R. L. Martin, K. Morokuma, V. G. Zakrzewski, G. A. Voth, P. Salvador, J. J. Dannenberg, S. Dapprich, A. D. Daniels, Ö. Farkas, J. B. Foresman, J. V. Ortiz, J. Cioslowski, D. J. Fox, *Gaussian 09 (Revision D.01)*, Gaussian, Inc., Wallingford, CT **2009**.

[48] A. Becke, *Phys. Rev. A* **1988**, *38*, 3098–3100.

[49] A. Becke, *J. Chem. Phys.* **1993**, *98*, 5648–5652.

[50] C. Lee, W. Yang, R. Parr, *Phys. Rev. B* **1988**, *37*, 785–789.

[51] a) L. N. Santagata, F. D. Suvire, R. D. Enriz, J. L. Torday, I. G. Csizmadia, *J. Mol. Struct. (Theochem)* **1999**, *465*, 33–67; b) L. N. Santagata, F. D. Suvire, R. D. Enriz, *J. Mol. Struct. (Theochem)* **2000**, *507*, 89–95; c) L. N. Santagata, F. D. Suvire, R. D. Enriz, *J. Mol. Struct. (Theochem)* **2001**, *536*, 173–188.

[52] C. Gonzalez, H. B. Schlegel, *J. Chem. Phys.* **1989**, *90*, 2154–2161.

[53] C. Gonzalez, H. B. Schlegel, *J. Chem. Phys.* **1990**, *94*, 5523–5527.

[54] P. Politzer, D. G. Truhlar, in *Chemical Applications of Atomic and Molecular Electrostatic Potentials*, Plenum Publishing, New York **1991**, p. 749.

[55] S. Portmann, H. Lüthi, *Chimia* **2000**, *54*, 766–770.

[56] E. Pettersen, T. Goddard, C. Huang, G. Couch, D. Greenblatt, E. Meng, T. Ferrin, *J. Comput. Chem.* **2004**, *25*, 1605–1612.